JOURNAL OF CATALYSIS 144, 50–59 (1993)

Peculiarities of Nickel Oxide Structure Transformation upon CO Hydrogenation

I. Initial Period of Catalyst Activation

O. S. MOROZOVA,* G. N. KRYUKOVA,†,[1] A. V. ZIBOROV,† and L. M. PLYASOVA†

*Institute of Chemical Physics of Russian Academy of Sciences, ul.Kosygina 4, Moscow 117334, Russia; and †Boreskov Institute of Catalysis of Siberian Branch of Russian Academy of Sciences, prospekt Lavrentieva 5, Novosibirsk 630090, Russia

Received October 19, 1992; revised April 28, 1993

A study has been made of the effect of nickel oxide morphology on the mechanisms of structural transformation during activation in a CO/H_2 environment using *in situ* X-ray powder diffraction and transmission electron microscopy. It was found that in the initial reaction stage nickel oxide structure transforms in two ways: (i) reduction of NiO to Ni with the formation of Ni/NiO system; and (ii) carbidization of NiO with the development of Ni_3C/NiO catalyst. The specific phase transition has been shown to depend on the structural similarity between the crystal lattices of the parent oxide and resulting product. The obtained data revealed that interaction of NiO with CO/H_2 reaction mixture is a structure sensitive reaction. The role of carbon monoxide in both topochemical processes is also discussed.

INTRODUCTION

Ni-based catalysts are typical catalysts for methanation reaction. Usually, these are supported systems or alloys containing Ni as well as metallic catalysts like Raney nickel (*1–5*). Although the methanation reaction has been the subject of much research, information on the phase transition of Ni-based catalysts under reaction conditions was, until recently, quite poor.

The aim of the present study was to investigate nickel catalyst structure formation on the first step of its treatment with a reaction mixture. Two NiO specimens prepared by different methods and possessing unequal morphologies have been studied. Structural investigation was carried out using *in situ* high-temperature X-ray diffraction (XRD) and transmission electron microscopy (TEM).

[1] To whom correspondence should be addressed.

EXPERIMENTAL

The first NiO(I) sample was prepared by the decomposition of $Ni(NO_3)_2$ solution at arc plasma (*6*). It has a BET specific surface area of 20 $m^2 g^{-1}$. The second NiO(II) specimen was obtained by air calcination of $NiCO_3$ (Merk Trademark) at 700°C for 5 h (the BET surface area is equal to 4.9 $m^2 g^{-1}$). X-ray microanalysis revealed[2] that carbon was present on the order of 0.01 and 0.004 wt% in the NiO(I) and NiO(II) samples, respectively.

X-ray spectra were obtained with a D-500 Siemens diffractometer fitted with an HTK-10 Anton Paar thermochamber for *in situ* investigation. The monochromatized CuK_α radiation was used as an X-ray source. Phase composition of the samples has been verified using JCPDS data files.

[2] Data were obtained using X-ray electron probe microanalyzer "Spectrozond" (Baikov Institute of Metallurgy, Moscow).

0021-9517/93 $5.00

Before X-ray measurements, 0.2 g of NiO sample was inserted into the thermochamber and heated in flowing He up to the chosen temperature. Then He was replaced by the reaction mixture ($CO : H_2 = 1 : 1$) with a flow rate ca. 80 ml min^{-1}. The experimental temperature interval was 195–240°C. The experimental recorded time was not less than 170 min. Registration velocity of X-ray spectra was equal to 0.5° min^{-1}.

For study of phase transformation kinetics the $2\Theta = 85°–95°$ spectral region was systematically investigated. This region is characterized by the simultaneous presence of diffraction peaks of different phases, namely, (400) NiO, (311) Ni, and (112) Ni_3C with 8, 20, and 80% intensities, respectively. The (511) X-ray diffraction peak of Ge powder used as the internal standard is also located in the same spectral region.

Analysis of X-ray diffractograms has made possible a direct observation of the catalyst structural transformation caused by the reaction mixture treatment. The following parameters of X-ray spectra for initial oxide and new phases have been taken into account: interplanar distances and unit cell parameters, particle sizes (*7*), and integrated intensities of diffraction peaks for the determination of a relative concentration of different phases in the specimens in question. For discrimination of the thermal effect (*7*) additional X-ray measurements for all the specimens were carried out in air and in He at the experimental temperatures. The alteration rates of different phase concentrations under reaction conditions were measured as a change of the integrated intensity of the characteristic diffraction peaks for the definite phase per time. For comparative analysis of the phase transition dynamics, the reduction of the NiO specimen by a mixture of 5% H_2 in He under analogous conditions was also studied.

The morphology and structure of the catalyst particles on the different steps of phase transition were analyzed *ex situ* using TEM. The resolution limit of the JEM-100CX microscope is above 0.3 nm. The specimens for TEM investigation were prepared according to the method described in (*8*).

RESULTS

NiO(I) Sample

According to TEM data, the particles of the NiO(I) sample have the form of cubic microcrystals with (100) as the most developed plane (Fig. 1a). The particle size is about 40 nm, but larger crystals (up to 200 nm) also exist.

Treatment of NiO(I) in reaction mixture has resulted in NiO reduction to metallic Ni and formation of a biphase Ni/NiO system. On the first reduction step at 195°C, the metastable Ni metal phase has been observed on X-ray spectra: the (311) Ni weak broadening diffraction peak appears and disappears periodically on diffractograms. At 210°C, the phase of Ni metal is reliably detected (see Fig. 2a), though not more than 8% of the NiO is reduced to metallic Ni. The latter was calculated using X-ray diffraction data, i.e., on the base of the alteration of the integrated intensity of the (400) NiO peak. According to TEM, on this stage the epitaxial growth of Ni metal on the surface of NiO particle with $[100]_{Ni}/[100]_{NiO}$ orientation relationship is observed. This result was obtained on the basis of Fourier analysis of the high resolution micrograph represented in Fig. 1c. Figure 1d shows Fourier transform pattern. One can see that there are diffraction spots indicated in the Fourier transform pattern with distances of 2.086 and 1.76 Å. These values are close to the (200) interplanar distances for NiO and Ni, respectively. It seems likely that metallic nickel arises in the form of a thin layer partially covering the surface of NiO microcrystal. The presence of metallic pieces on the oxide surface is also confirmed by the observation of moiré fringes on the micrograph (see Fig. 1c) due to the slight discrepancy between the lattice parameters of Ni oxide and Ni metal.

As derived from X-ray measurements, the particle size of Ni in the sample under inves-

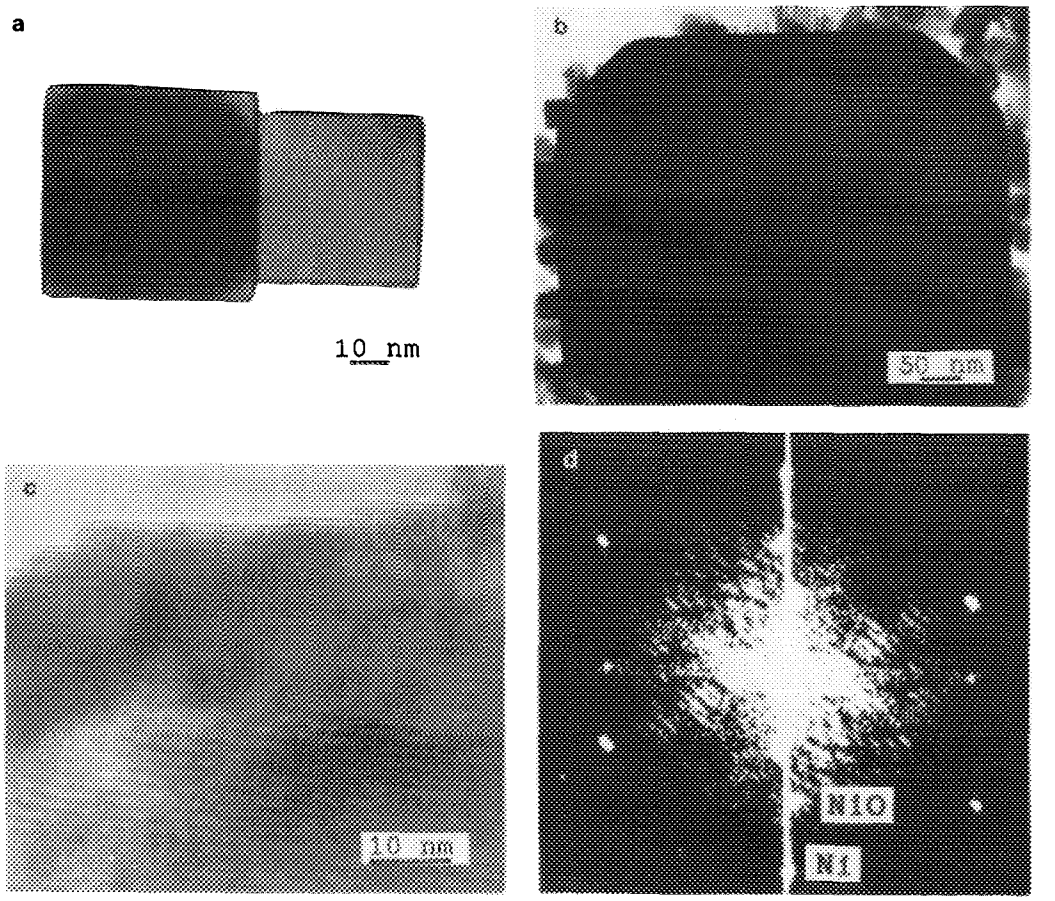

FIG. 1. TEM micrographs of (a) the initial NiO(I) particle, (b) NiO(I) microcrystal on the first reduction step, and (c) NiO(I) particle partially reduced to Ni metal; (d) Fourier transform pattern of the micrograph represented in (c).

tigation increases with increasing concentration of metal phase when raising the temperature (from 20 to 50 nm at 210°C and up to 60 nm at 240°C).

Figure 3 shows the integrated curves of NiO(I) reduction by reaction mixture of CO in H_2 (1 : 1) at 210°C (curve (1)) and at 240°C (curve (2)), respectively. For comparison, the curve of NiO(I) reduction by mixture of 5% H_2 in He at 210°C is also given in Fig. 3 (curve (3)). It should be noted that experiments at 210 and 240°C were carried out successively. After reduction at 210°C the specimen was cooled to room temperature in a CO/H_2 mixture which was replaced by He. After 12 h, the specimen was heated up to 240°C in 7 min, then a reaction mixture was introduced.

From Fig. 3, one can see that the process of NiO(I) reduction in the CO/H_2 mixture is characterized by a prolonged induction period (ca. 30 min). In contrast, the reduction process in the H_2/He mixture may be described using classic topochemistry equations, in agreement with models reported in (9). After 30 min, the NiO reduction rate in H_2/He became higher than that in the CO/H_2 mixture (ca. 3.5-fold increase). Consequently, CO may be considered as an inhibitor of the reaction of NiO reduction.

Configurations of curves (1) and (2) from Fig. 3 indicate the diffusion type of NiO

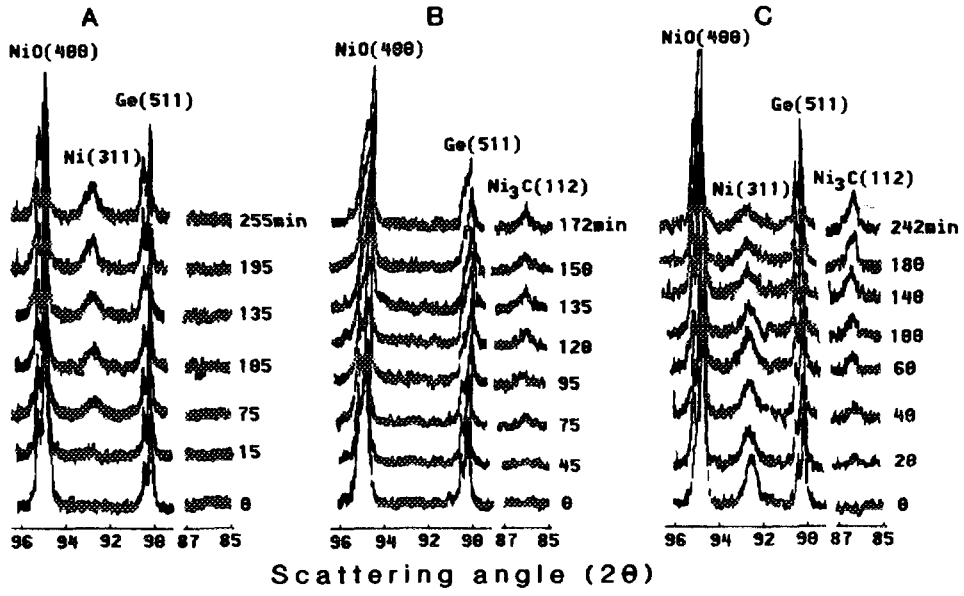

FIG. 2. X-ray spectra obtained during nickel oxide structure transformation under treatment with CO/H_2 reaction mixture: (a) NiO(I) sample, 210°C; (b) NiO(II) sample, 240°C; (c) $Ni_3C/Ni/NiO(II)$ system, 240°C.

reduction mechanism. Indeed, the rate of Ni formation falls right on the line. For drawing these curves, we used $(W - 1/\sqrt{t})$ coordinates, where W (rate of Ni formation) was calculated on the basis of alteration of the integrated intensity of the (311) X-ray diffraction peak for experimental time t. The latter was considered as a period from the beginning of each step on the kinetic curves (9). Steps on the (1) and (2) kinetic curves seem to be associated with the reduction of the definite amount of NiO. These data are listed in Table 1.

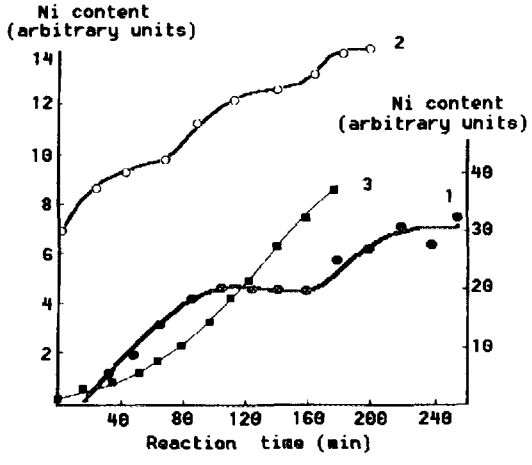

FIG. 3. Integrated kinetic curves of Ni metal formation from NiO(I) specimen under different experimental conditions: (1) 210°C, $CO/H_2 = 1:1$; (2) 240°C, $CO/H_2 = 1:1$; (3) 210°C, 5% H_2 in He.

Data given in Table 1 show that reaction rate decreases just after the formation of 4–6% of the metallic Ni. Afterwards new

TABLE 1

Degree of NiO(I) Reduction to Ni Metal on Different Steps of Oxide Interaction with the CO/H_2 Reaction Mixture

Temperature (°C)	Experimental time (min)	Initial step of NiO reduction (%)	Final step of NiO reduction (%)
210	153	First step 4.6	Second step 7.6
240	57	First step 14	Third step 22
	122	Second step 18	

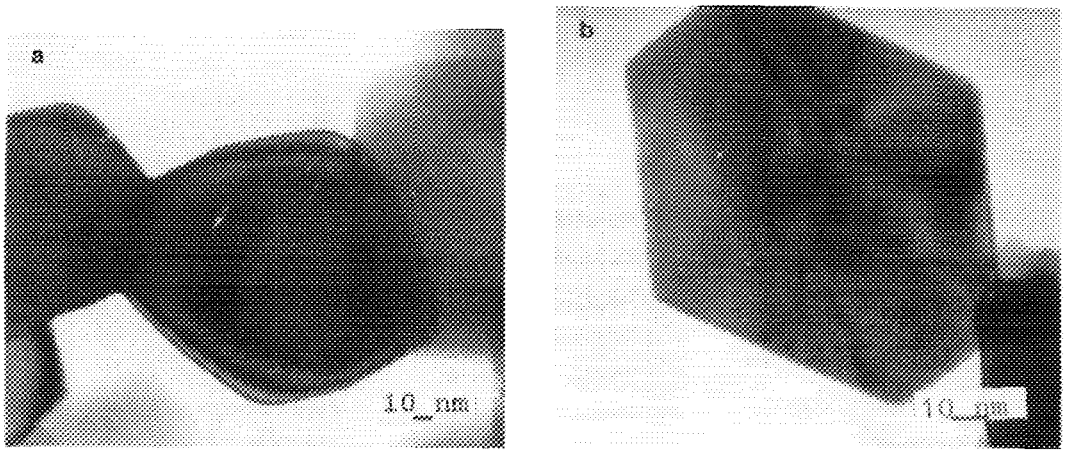

FIG. 4. TEM micrographs of NiO(II) sample on different stages of its reduction by Co/H_2 reaction mixture: initial (1), after carbidization (b).

a reactive surface forms at once, and the reduction process renews and proceeds until the reaction zone becomes full of products of the NiO interaction with the reaction media.

NiO(II) Sample

According to TEM results, particles of the NiO(II) specimen are in the form of platelets with (111) developed faces and sizes about of 150 nm (Fig. 4a). One can also observe NiO microcrystals with (110) well-developed planes and surface steps on the lateral sides of NiO particles.

In comparison to the NiO(I) sample, the temperature of NiO(II) transformation upon treatment by the reaction mixture is higher and equal to 240°C. The final product of such a transformation is a biphase Ni_3C/NiO system. The Ni metal phase is not observed (Fig. 2b). Furthermore, additional experiments were performed when the Ni metal phase was developed by reduction of NiO(II) with hydrogen. And then, after the following treatment with the reaction mixture under the same conditions as in the case of the Ni/NiO(I) system, this metal phase easily transformed into nickel carbide. But it should be noted that the Ni/NiO(I) catalysts did not transform into Ni_3C during the whole experimental cycle.

Figure 5 shows the integrated kinetic curves of NiO(II) carbidization by CO/H_2 mixture at 240°C. Curve (1) refers to Ni_3C formation, curve (2), to NiO consumption. As one can see, the configuration of these curves is the same as in the case of the formation of Ni metal from NiO(I). There is a diffusion controlled reaction, as evident from the linear character of the kinetic curves.

Figure 6 represents the rate of nickel carbide formation (curve (1)) and change of its crystal sizes (curve (2)) calculated on the

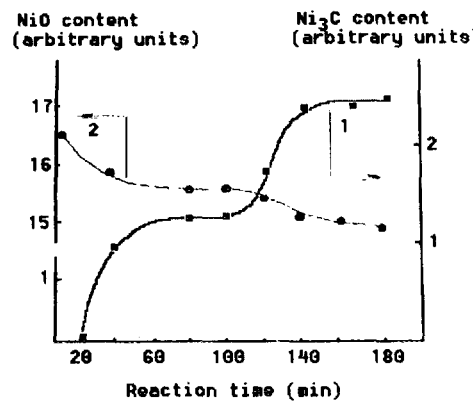

FIG. 5. Integrated kinetic curves of NiO(II) carbidization by CO/H_2 = 1 : 1 mixture at 240°C: (1) Ni_3C formation; (2) NiO consumption.

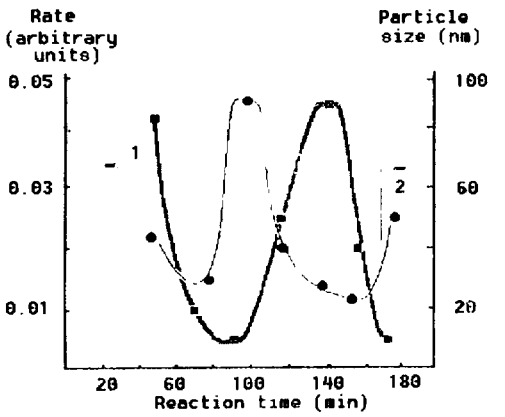

FIG. 6. Alteration of (1) the rate of Ni_3C formation and (2) Ni_3C particle sizes during the process of NiO(II) carbidization by CO/H_2 mixture at 240°C.

basis of X-ray measurements upon reaction conditions. As evident from this figure, a reaction decrease coincides with the increase of Ni_3C crystal sizes up to the largest ones. After that the reaction comes new cycle beginning with a sharp decrease of Ni_3C particle sizes. Calculations indicate that on the initial stage of NiO(II) carbidization (first step on curve (1)) only 47% of the nickel carbide is formed.

For the performance of the next reaction cycle (second step on curve (1) from Fig. 5) and formation of ca. 53% of the Ni_3C, ca. 6.5% of NiO(II) should be depleted. These calculations fit well with TEM data. According to TEM observation Ni_3C phase appears on the surface of the NiO(II) crystal in the form of regular hexagonal platelet (Fig. 4b). Such a platelet occupies a whole (111) surface of the NiO(II) particle, then it may release from the surface, thus promoting formation of a new Ni_3C microcrystal.

Figure 5 demonstrates a long induction period (over 40 min) for the carbidization process. The presence of such an induction period may be associated with the accumulation of a definite amount of active carbon in the oxide volume and approximation to the stoichiometric Ni/C ratio for the formation of the nickel carbide phase (*10*). To a certain extent, the above assumption might be justified by the fact that the NiO lattice parameters increase on the first stage of the carbidization process (Fig. 7) due to the insertion of active carbon into the oxide lattice.

DISCUSSION

With careful examination of represented results, it should be possible to reach some important conclusions. First, the interaction of CO/H_2 mixture with nickel oxide is a structure sensitive reaction. The mechanism of this reaction depends on the structure similarity between crystal lattices of the reagent and product, therefore, two routes of NiO structure transformation may be realized, namely, reduction of NiO to Ni metal and NiO transformation into Ni_3C. Second, the peculiarities of NiO structure transformation could not be reliably explained using a formal kinetic approach. Comparison between the shapes of curves from Figs. 3 and 5 indicates that the kinetics of NiO transformation into Ni metal (NiO(I) sample) and Ni_3C (NiO(II) sample) may be ascribed as diffusive. The reaction decrease for different routes of NiO transformation is associated with the blocking of the reaction surface. The structure transformation goes through a new reaction cycle after a new reactive surface becomes accessible for the

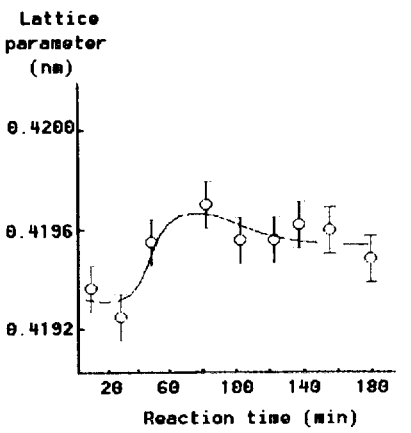

FIG. 7. Alteration of the (400) NiO lattice parameter during the carbidization of the NiO(II) sample.

reaction mixture. The rates of these topochemical processes seem to be equal. But mechanisms for both reactions essentially differ from each other.

For the NiO(I) specimen, the main factor responsible for the reduction process is thought to be Ni^{2+} cation diffusion from the bulk of the nickel oxide (*11*). This diffusion depends on the gradient of oxygen concentration on the oxide surface. The oxygen is removed from the surface due to interaction with hydrogen and/or carbon monoxide. We may suggest that on the first reaction step metal arises on the oxide surface in the form of small islands. The appearance and disappearance of the (311) Ni metal peak on X-ray spectra may be considered as evidence for the growth or destruction of such metal islands.

On the second reaction step, the epitaxial metal layer forms on the oxide surface as derived from the analysis of TEM micrographs (Fig. 1c). It should be noted that such a situation is realized during NiO(I) reduction by H_2/He mixture. But in this case the reaction rate as well as the degree of NiO transformation into metallic Ni is higher. Due to a broad size distribution in the NiO(I) specimen, the above-mentioned assumption is of relevance to the NiO crystals with mean sizes. Therefore, one could suggest that small NiO particles are covered by a "thick" metal layer, whereas more larger crystals only begin to reduce with formation of small metal clusters.

The peculiarities of NiO(I) reduction with CO/H_2 mixture were shown to be associated with the dramatic change of morphology of the oxide particles. TEM results revealed that on the first step of NiO(I) reduction with the CO/H_2 reaction mixture, there are small perfect cubic oxide microcrystals (size is above 2 nm) and large (up to 200 nm) ones with numerous surface steps (see Fig. 1b). According to data represented in (*12*) the surface reconstruction, recrystallization and destruction of the (100) plane of the NiO microcrystal may be caused by the presence of carbon clusters being formed in a subsurface layer of NiO particle at a low partial pressure of carbon monoxide. Indeed, the formation of the surface steps and facets in NiO(I) microcrystals was observed only after specimen treatment with CO/H_2 reaction mixture.

It is well established (*13*) that carbon monoxide actively reacts with the (100) plane of NiO monocrystal in the presence of hydrogen traces. As a rule (*14*), the concentration of point defects in the structure of NiO cubic crystals is high, therefore the scheme of carbon migration into the NiO subsurface layer can be written as

$$H_2 + O_{lat} \rightarrow H_2O + Vac,$$
$$CO + Vac \rightarrow O_{lat} + C_{intrinsic},$$

where O_{lat} is lattice oxygen, and Vac is a lattice vacancy or isolated Ni atom. Thus, the presence of CO may result in the destruction of large NiO(I) microcrystals on the first step of their interaction with reaction media.

On the next step of the reduction process when the metal phase forms on the oxide surface, the CO adsorption on the metal centers and metal–oxide boundary might take place as follows (*15*):

$$CO_{gas} + * \rightarrow CO^*_{ads}$$
$$CO^*_{ads} + CO^*_{ads} \rightarrow * + C^*_{intrinsic} + CO_2.$$

Here * designates the active site. This carbon seems to localize on the interphase metal–oxide boundary or to "fall" into the crystal volume with the formation of carbon clusters (*10, 16, 17*). The accumulation of carbon on the interphase boundary might change the diffusion characteristics of this region. The latter is essential because the intergrain boundary strongly affects the process of cation and oxygen diffusion (*18*).

Thus, we can easily see that carbon monoxide plays a key role in the topochemical process. On one hand, the dissociative adsorption of CO on the metal centers (a first stage of CO molecule activation in methanation reaction) leads to carbon insertion into the metal–oxide boundary that might en-

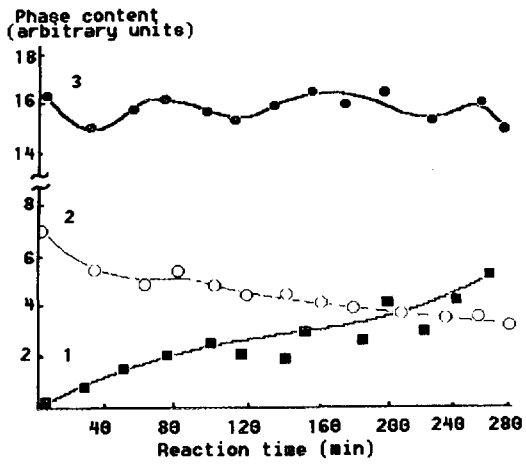

FIG. 8. Integrated kinetic curves of Ni/NiO(II) carbidization by CO/H_2 = 1 : 1 at 240°C: (1) – Ni_3C; (2) – Ni; (3) – NiO(II).

hance the oxide reduction process. On the other hand, carbon easily diffuses through the bulk of the NiO microcrystal with formation of carbon clusters; the latter may result in the development of surface steps and destruction of the oxide particles. It seems likely that steps are the fresh surface on which the process of NiO reduction to Ni metal renews at a time and continues until the surface of the largest NiO crystals becomes reactive.

Results of XRD measurements which can reveal an average unit cell indicate that not more than 25% of NiO(I) reduces to Ni metal. Consequently, all structural transformations occur at the NiO subsurface layer. Taking into account the value of the sample specific surface, mean particle diameter, and geometry of the unit cell of NiO, we may calculate the thickness of this layer. The latter does not exceed a threefold unit cell parameter. It seems likely that the amount of carbon accumulated at the NiO subsurface during the time for reduction of 40–60% of the NiO(I) (see Fig. 3, steps on curves (1) and (2)) is enough for the creation of the destructive strains in the crystal lattice.

The interaction of the NiO(II) catalyst with the CO/H_2 reaction mixture shows a difference with respect to the NiO(I) sample. In this case only a nickel carbide phase has been observed. Neither TEM nor XRD method revealed the presence of Ni metal in the NiO(II) specimen. When the Ni/NiO(II) biphase system was specially prepared, the Ni metal easily transformed into Ni_3C after its interaction with CO/H_2 at 240°C (Fig. 8). We emphasize that in the case of the Ni/NiO(I) system Ni_3C has not been obtained under the same experimental conditions.

The observed direction of the topochemical reaction may be associated with the structure similarity between the (111) most developed face of the NiO(II) sample and the (0001) plane of the hexagonal unit cell of Ni_3C (see Fig. 9). Although there is no obvious evidence, the transformation of NiO into the Ni_3C may be realized via the intermediate phase of Ni metal with hexagonal crystal lattice. It is known (*19*) that lattice parameters of Ni_3C are similar to the same characteristics of the hexagonal modification of Ni metal which might exist in the epitaxial form on the (111) face of NiO.

In accordance with previous results (*10*), the formation of nickel carbide requires accumulation of a stoichiometric amount of carbon at the subsurface layers of nickel oxide. Indeed, in our experiments the prolonged induction period of the carbidization reaction (ca. 40 min) as well as the increase of the NiO lattice parameter were really observed (Fig. 7). In comparison with the NiO(I) sample, the temperature of NiO(II) transformation under treatment by the CO/H_2 reaction mixture is higher. This differ-

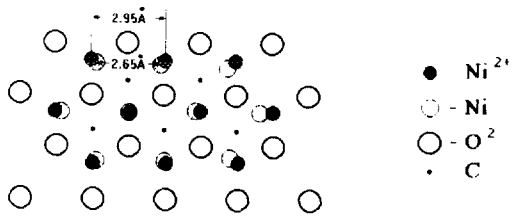

FIG. 9. Structure similarity between the (111) plane of NiO and the (0001) plane of Ni_3C.

ence should be derived (a) from the difficulty of CO and H_2 molecule activation on the (111) plane of NiO, and (b) from the low concentration of the surface imperfections, i.e., steps as in the case of NiO(I) particles.

As mentioned above, due to the structural similarity between cubic unit cells of nickel oxide and metal, a thin epitaxial metal layer forms on the (100) face of the microcrystal of the NiO(I) sample. Carbon could not react with the (100) plane of NiO(I) and might only destroy oxide microcrystals. We are concerned with another situation in the case of the NiO(II) specimen. At first, carbon easily reacts with the (111) face of the NiO crystal which possesses structural similarity to the (0001) plane of hexagonal Ni_3C. Thus forming platelets of Ni_3C occupy the whole surface of NiO microcrystal. On the next reaction step, the Ni_3C platelets loosen a contact with "parent" NiO particles, as evident from TEM data (Fig. 4b), a new fresh surface of NiO becomes accessible for the formation of another Ni_3C platelet, and the carbidization reaction renews.

SUMMARY

The structure peculiarities of parent oxide microcrystals substantially affect the process of formation of nickel-based catalysts for methanation reaction upon reaction conditions. The direction of the topochemical reaction is highly sensitive to the structural arrangement of the most developed faces of the catalyst particles. In the course of our investigations, it became clear that there are two possible routes of interaction of nickel oxide with the CO/H_2 reaction mixture, namely, reduction of NiO to Ni metal and NiO transformation into Ni_3C. In the first case, a Ni/NiO biphase catalyst which consists of the stepped oxide microcrystals covered by thin epitaxial layers of Ni metal is formed from parent oxide particles with the (100) developed faces. Carbon monoxide plays a significant role in the formation of the unusual morphology of catalyst particles. In the second case, NiO is transformed directly into Ni_3C because the (111) most developed faces of the parent oxide have a structural similarity to the (0001) plane of the hexagonal nickel carbide phase. As a result, a catalyst for methanation reaction represents the Ni_3C/NiO system.

Kinetics of the reduction and carbidization processes are similar. But only complex physical and chemical investigation has been able to highlight the mechanism of these topochemical reactions and to confirm their structure sensitivity.

ACKNOWLEDGMENTS

We acknowledge Dr. P. N. Tsybulyov (Institute of General and Inorganic Chemistry, Kiev) for providing the plasmochemical NiO sample. We are also grateful to Professor A. Ya. Rozovskii (Institute of Petrochemical Synthesis, Moscow) and Dr. V. A. Sadykov (Boreskov Institute of Catalysis, Novosibirsk) for valuable comments and useful discussions.

REFERENCES

1. Weatherbee, G. D., and Bartholomew, C. H., *J. Catal.* **68,** 67 (1981).
2. Ozdogan, S. Z., Gockis, P. D., and Falconer, J. L., *J. Catal.* **83,** 257 (1983).
3. Yokoyama, A., Komiyama, H., Inoue, H., Masumoto, T., and Kimura, H. M., *J. Catal.* **68,** 355 (1981).
4. Hayes, R. E., Thomas, W. J., and Hayes, K. E., *Appl. Catal.* **6,** 53 (1983).
5. Hupp, J. M., Edmond, I. K., and Wagner, N. J., Chem. Comm. **2,** 94 (1983).
6. Parkhomenko, V., and Tsybulyov, P. N., *in* "Proceedings, 8th International Symposium on Plasmochemistry, Tokyo," Vol. 4, pp. 2105–2110 (1987).
7. Mirkin, A. I., "Handbook on X-ray Diffraction Analysis of Polycrystals." Nauka, Moscow, 1961. [in Russian].
8. Kryukova, G. N., Zaikovskii, V. I., Tikhov, S. F., Sadykov, V. A., Popovskii, V. A., and Bulgakov, N. N., *J. Solid State Chem.* **74,** 191 (1988).
9. Rozovskii, A. Ya., "Catalyst and Reaction Media." Nauka, Moscow, 1988. [in Russian].
10. Darling, G. R., Pendry, J. B., and Joyner, R. W., *Surf. Sci.* **221,** 69 (1989).
11. Atkinson, H. V., *in* "Advances in Ceramics" (C. R. A. Catlow and W. C. MacKroad, Eds.). Am. Ceram. Soc., Westerville, OH, 1987.
12. Buckett, M. I., and Marks, L. D., *Surf. Sci.* **323,** 353 (1990).

13. Boudriss, A., and Dufour, L. C., *in* "Non-stoichiometric Compounds. Surfaces, Grain Boundaries and Structural Defects" (J. Nowotny and W. Weppner, Eds.), p. 311. Kluwer, London/New York, 1989.
14. Kryukova, G. N., Thesis, Moscow, 1989.
15. Rosei, R., Giccacci, F., and Mariani, C., *J. Catal.* **83,** 19 (1983).
16. Joyner, R. W., Darling, G. R., and Pendry, J. B., *Surf. Sci.* **205,** 513 (1988).
17. Allen, V. M., Jones, W. E., and Pacey, P. D., *Surf. Sci.* **220,** 193 (1989).
18. Atkinson, H. V., *Oxid. Met.* **24,** 177 (1981).
19. Jonson, M. E., and Moss, R. L., *Acta Crystallogr.* **21,** 1004 (1966).